Article

Gloss Level, Type of Paper and Colour of HDF Boards Finished with the Energy-Saving Acrylic Paint System

Milena Henke [1], Tomasz Krystofiak [1,*], Emilia Adela Salca [2,*] and Barbara Lis [1]

1 Department of Wood Science and Thermal Techniques, Faculty of Forestry and Wood Technology, Poznan University of Life Sciences, Wojska Polskiego 28, 60-627 Poznan, Poland; milena.henke@up.poznan.pl (M.H.); barbara.lis@up.poznan.pl (B.L.)
2 Faculty of Furniture Design and Wood Engineering, Transilvania University of Brasov, Universitatii 1, 500068 Brasov, Romania
* Correspondence: tomasz.krystofiak@up.poznan.pl (T.K.); emilia.salca@unitbv.ro (E.A.S.)

Abstract: The global drive to eliminate mercury is stimulating the development of LED lamps for UV curing of coatings. Despite its many advantages, the transition to this system in the furniture industry presents technological issues. This paper aimed to determine the impact of the paint line's individual technological and process parameters on the coating's optical properties, such as colour and gloss of furniture components made of white-coloured light-weight boards. Samples were prepared under the conditions of an industrial paint line using LED and traditional mercury lamps at the rate of 50 m/min. The colour was tested using the CIELAB system on a BYK GARDNER spectrophotometer, while the gloss was measured using the PICO GLOSS meter. Based on the data obtained, the optical parameters were found to be highly stable irrespective of the power drop in the LED lamps. The coordinates L*, b* and gloss G were affected by the amount of topcoat and basecoat, the number of coats, the mercury lamps' power and the panel grinding programs used. The results of the tests showed that high L* and b* values could be achieved by increasing the number of overlays. This solution also ensures less basecoat and topcoat consumption, contributing to large material savings.

Keywords: UV lacquer system; LED radiators; high-density fibreboard; colour measurements; gloss level

1. Introduction

The global paint products market is estimated to be worth USD 248.87 billion in 2023. Over the next five years, the market is projected to grow to USD 326.09 billion at a 7% CAGR [1]. Such a thriving industry is stimulated by global challenges, especially in the area of ecology [2]. The demand for environmentally friendly coatings is driven by the increasing awareness of consumers who expect sustainable products. Regulations that have been introduced in the United States, China and European countries are intensifying the efforts of entrepreneurs to implement low-emission technologies using organic compounds [3,4]. The use of UV varnishes is a good alternative to solvent-based varnishes in the protection of wood and wood–plastic surfaces [5,6]. The wood industry is the largest market segment for UV technology. In 2019, it accounted for 43% of the total UV curing market, and China proved to be the largest consumer. Asian countries are cited as the region where UV technology is developing most rapidly [2,3,7]. Over the years, UV-curable coatings have evolved, allowing them to be used in a wide variety of applications, such as automotive, biomedical, electronics and adhesive processes [6,8–10]. UV lamp-curing technology is considered an efficient process due to shorter curing times [11–15].

The coating process involves the conversion of functional monomers into a cross-linked polymer using free radicals under the influence of UV radiation [11–13]. Mercury lamps constitute the basis of UV curing technology. Ultraviolet, visible and infrared wavelengths are emitted due to the evaporation of mercury into plasma at high temperatures [16].

Gallium-doped mercury lamps are used for thick, pigmented coatings [17]. The disadvantages of curing technology using mercury lamps should, however, be mentioned. Only 5% of the energy is used to cure the varnish, while the rest is converted into heat, which raises the surface temperature, risking the flow of resins onto the wood surface and posing a fire hazard [18–24]. Furthermore, depending on its length and design, the lamp may contain between 10 and 100 mg of mercury. When adequately transported and operated, it poses no risk. Their recycling must, therefore, be based on the safe extraction of mercury and its transfer to sustainable disposal, storage or further processing [16]. International policy is leaning towards reducing this element in the environment. Global mercury consumption is high, at around 3,600 tonnes per year, though there has been a slight decrease from previous decades [25]. There are many regulations, e.g., REACH and the TSCA/Lautenberg Act, as well as regulatory bodies, e.g., the United States Environmental Protection Agency and the United Nations Environment Programme, which aim to create consumer awareness and accelerate the changes taking place in the industry. The most frequently cited document on the circulation of mercury is the European Commission's RoHS2 Directive. Currently, the exemption for the use of Hg in the manufacturing of UV curing lamps has been extended from 2021 to 2027 [16,26–28]. In 2017, the Minamata Convention international treaty was ratified by 137 countries. This does not prohibit the use of mercury in the manufacturing of UV lamps but mandates all member states to limit the use of mercury [29,30].

An alternative to high-energy mercury lamps are LED lamps, known since the mid-2000s. No mercury is used in their manufacturing, and their operation does not generate ozone [26]. LED radiation sources are based on semi-conductor components that, when energized, emit a narrow band of UVA energy [31,32]. The highest recorded temperatures during curing are 60 °C, about six times lower than in the case of mercury lamps. Air cooling of the LED lamps is unnecessary, resulting in lower sound levels. With LED lamps, coatings can be cured on resinous (pine, fir, spruce) or oily (mahogany) wood substrates and glued veneers. High energy efficiency, instant lamp activation/de-activation and elimination of lamp warm-up times generate electricity savings of 45–60%. The lifetime of LED lamps is predicted to be 10,000–20,000 h, with a 5% drop in performance over this time. Compared with conventional mercury lamps, the operating time is around 500–2000 h, and the power reduction at the end of life is around 50% [17,21,33,34]. UV LED technology's undoubted disadvantage is the coating's lower degree of cross-linking [35]. Finished product manufacturers seeking to increase production efficiency increasingly reduce curing times by increasing line speeds. However, this raises some problems with the cross-linking of paint products. Therefore, combined technologies are used in combination with conventional lamps. Lower line speeds were confirmed to provide a higher degree of curing [36]. Due to the efforts to maximize line efficiency, researchers are looking for suitable acrylate amine oligomers that allow the desired coating cross-linking to be achieved [37]. Intensive work is also underway on LED lamps with higher intensity and in the UV-B and UV-C spectrum [38]. The use of LED lamps involves the risk of failure of individual diodes. This, in turn, carries the risk of insufficient curing control. If the issue is not identified during manufacturing, the customer is exposed to residual monomers, photoinitiators and other harmful ingredients. The development of Industry 4.0 requires the definition of precise process requirements [39]. Thanks to the integrated sensors in the illuminator (e.g., bulb temperature, air temperature, UV intensity, humidity, air pressure), the Advanced Intelligent Monitoring System (AIMS) can transfer data to a cloud-based environment to co-create Industry 4.0. An intelligent IoT-enabled UV system provides real-time process performance data and allows analysis for predictive diagnostics [40].

One important aspect that determines the attractiveness of the finished products is their optical properties, such as colour and gloss. Many researchers have described the issue of obtaining the right gloss. After many years of the popularity of high-gloss coatings, matt surfaces are attracting increasing interest [41]. UV-cured coatings exhibit higher gloss values than other technologies [42]. New varnish formulations are being developed to provide a higher matt finish. Achieving good matting is about finding the right amount

of matting agent, reactive ingredients and application and curing parameters. It has been proven that a high photoinitiator level, a high line speed and a high dose of UV light reduce the matting effect [41]. Roller application also produces a higher gloss than spray application [43]. Low substrate roughness, coating thickness and number of layers are all factors that affect the coatings' optical properties, and UV coatings turned yellow in aging tests [44,45].

Repeated reports in research about the lack of adequate coating curing with LED lamps and issues with optical properties at high line speeds provided the impetus to address the topic. Despite increasing pressure to implement LED-based UV curing technology, it still lacks clear coating curing procedures [16,46]. The challenge is determining the impact of technological parameter combinations that ensure adequate coating cross-linking and high final quality.

The analysis of the available literature includes studies, only fragmentarily connected with the signalled subject matter. This is mainly due to the fact that achievements of this kind are covered by the highest confidentiality clause. Therefore, it was decided to study the optical properties of varnish coatings obtained in industrial conditions to control the parameters of the technological process of surface finishing.

This paper aims to determine the impact of fibreboard (HDF) density, grinding parameters, the amount of basecoat and topcoat applied, the number of coats and different lamp powers on a combined industrial line using LED and mercury lamps at 50 m/min. It was assumed that these factors could significantly impact the coating's resistance and that simply learning about them and identifying the relationship could support entrepreneurs and manufacturing technologists and become a starting point for further work on varnish formulations and LED lamps.

2. Materials and Methods

2.1. Materials

The board used for the study was a frame version with a honeycomb core of $700 \times 390 \times 22$ mm. The frame was made of 17 mm thick particleboard with a density of $540 +/- 20$ kg/m^3 (Kronospan, Szczecinek, Poland). The 2.5 mm thick HDF boards from two different manufacturers, known as A and B, were used as the cladding material (Table 1). The total number of samples used for the experiments was 198.

Table 1. Primary characteristics of HDF boards.

Parameter	Board Marking	
	A	**B**
Density [kg/m^3] acc. to DIN EN 323:1993	850	830
Modulus of elasticity [MPa] acc. to the DIN EN 310:1993 standard	4300	4500
Moisture content [%]	7	7
Swelling resistance [%] acc. to the DIN EN 317:1999 standard	45	45

A one-component PVAC adhesive with a viscosity of 14,000 mPa·s indicated with a METLER TOLEDO S210 meter at 40 ± 0.5 °C and a pH of 4.1 was used to adhere the chosen boards together. After a conditioning period of 96 hours, the structures with a 22 mm thickness were subjected to finishing. Putty, basecoat and topcoat paint were used in a multi-layer paint scheme (Table 2).

2.2. Surface Varnish Finishing Process

Before the application of varnish products, the HDF boards were sanded using 180–220 and 220–220 sanding paper, after which the boards were passed through the rollers. The resulting varnish coatings consisted of 5 and 6 applied layers. The individual coatings were cured with 120, 90 and 60 W/cm^2 mercury lamps and 12, 9 and 6 W/cm^2 LED

lamps. Before basecoat application, intermediate sanding was performed with 220–220 and 400–400 sanding paper. Finally, nine variants in white were prepared for experiments (Table 3). The finishing process was done under technological conditions on a prototype paint line.

Table 2. Primary physicochemical characteristics of varnish products.

Parameter	Heavy Putty	Basecoat	Topcoat
Density [g/cm^3]	1.63 ± 0.15	1.73	1.30 ± 0.15
Solids content [%] acc. to the PN-EN ISO 3251:2019 standard	95.3 ± 0.5	98.3 ± 0.5	97.8 ± 0.5
Viscosity [mPa·s] (Brookfield, Thermosel 35 °C, 20 rpm, spindle 27)	7700	400	1475

Table 3. Amounts of varnish application.

Type of Varnish Product—UV Acrylic	Amount of Applied Varnish [g/m^2]								
heavy putty	50	50	50	50	50	50	50	50	50
basecoat	40	45	50	40	45	50	40	45	50
topcoat	3	3	3	6.5	6.5	6.5	10	10	10

Figure 1 shows a schematic line for finishing boards with UV varnish products. In the first step of the process, the parts were sanded and then two layers of putty were applied. The first was cured with 1 mercury (Hg) lamp, while two Hg lamps were used to crosslink the second layer. The next operation was to sand the surface of the putty and apply the basecoat as two layers. Each layer was cured using two LED lamps. Some variants were prepared with three coats of basecoat. In the final step, a topcoat was applied and cured using two LED lamps and five mercury lamps. All operations were performed on the production line at a speed of 50 m/min at ambient temperature.
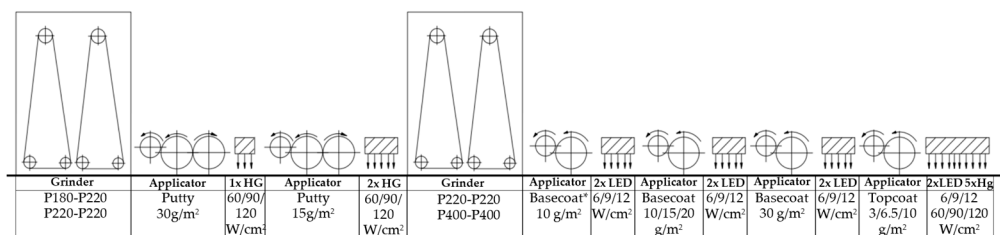
Figure 1. An overview of the varnish line on which the tests were conducted.

2.3. Gloss Measurement

Using a PICO GLOSS 503 photoelectric apparatus, the gloss was measured following the DIN 67530:1982 and ISO 2813:1994 standards [47,48]. Six measurements were taken for each sample in the direction opposite the varnish application using 60-degree geometries on each sample.

2.4. Colour Measurement

The colour was measured with the BYK GARDNER instrument. According to the ISO 7724-2 standard, six colour measurements were taken for each sample in the opposite direction to the varnish application [49]. The colour was assessed using the CIELab system. The following characteristics were used to measure colour: lightness (L*), degree of redness (a*) and degree of yellowness (b*). Because red and green are opposite colours and blue and yellow are complementary colours, the colour axes (a* and b*) are based on this idea.

The values on each axis range from positive to negative. Positive numbers on the a-a' axis represent amounts of red, whereas negative values represent amounts of green. Yellow is positive and blue is negative on the b-b' axis. Zero represents neutral grey for both axes. Lightness (denoted as L*) is represented by the central vertical axis, with values ranging from 0 (black) to 100 (white). A grid of lines parallel to the a* and b* axes surround planes of constant brightness L* in the graphic depiction of this colour space [50].

2.5. Processing Data

The test findings were analysed using the Minitab 19 and Microsoft Excel programs. The normality of the distribution was examined, and an analysis of variance (ANOVA) was carried out, to determine the impact of various parameters on the colour and gloss of the surface. The data were displayed using the main effects chart. A prediction and optimization report was produced.

3. Results

3.1. Initial Statistical Analysis

The normal distribution hypothesis was verified using the Ryan–Joiner test, similar to the popular Shapiro–Wilk test. At a significance level of $\alpha = 5\%$, the collected brightness L*, b* colour coordinate and gloss G data were normally distributed for the raw data. The null hypothesis that the error variance of the dependent variable was equal in all groups was assumed at the fixed confidence level (>0.05). The exception was the parameter a*, its data did not present a normal distribution and the null hypothesis was rejected [51].

ANOVA analysis was performed. The data were evaluated based on six variables: density of high-density fibreboard (HDF), sand belt used during sanding, amount of basecoat and topcoat applied, number of coats, different UV mercury lamps and different UV LED lamp powers used to cure the surface of coating (Table 4). It was found that the mean gloss level values differed at a significance level of $\alpha = 0.05$ for UV mercury lamp power W/cm, amount of topcoat, number of applicators and sandpaper. In the case of brightness L* and colour b*, the parameters related to the varnish application process (amount of topcoat and basecoat, number of applicators) were statistically different at $\alpha = 0.05$. The other factors examined had no statistically significant effect on the coating's optical parameters considered in the paper.

3.2. Colour Coordinates

The results obtained were further statistically analysed. Figures 2 and 3 show Pareto effect size plots in standard deviation for coordinates L* and b*. The most influential factors (larger than 2) were the number of applicators used and the amount of topcoat applied, followed by the amount of the basecoat applied. The sandpaper used was the factor in the intermediate importance group. Figure 2 also shows the main effect plot for the factors studied. Increasing the number of varnish applicators resulted in higher coordinates of L* and b*. An increase in brightness was noted during the increase in application when the topcoat and basecoat were applied. The finer the abrasive grit size (220–220 and 400–400), the higher the coating performance. The type of board was first in the group of factors with the least impact on L* and b*. Board A, with higher density, achieved higher brightness. For UV mercury and LED lamp power, the line is horizontal (parallel to the *x*-axis), so there was no main effect. Each level of the factor affected the response similarly, and the response mean was the same across all the factor levels.

Table 4. One-way ANOVA analysis of gloss as a function of the process variables.

One-Way ANOVA Response	Source	DF The Total Degrees of Freedom	Adj SS Adjusted Sums of Squares	Adj MS Adjusted Mean Squares	F-Value	*p*-Value
G.	UV LED lamp power W/cm	2	0.55	0.2756	0.01	0.991
	UV mercury lamp power W/cm	2	216.7	108.36	3.90	0.022
	Amount of topcoat	2	3426	1712.96	152.20	0.000
	Amount of basecoat	2	75.06	3753	1.32	0.271
	Number of applicators	1	504.0	504.04	19.25	0.000
	Type of board	1	9.69	9.689	0.34	0.562
	Sandpaper	1	646.6	646.63	25.41	0.000
L*	UV LED lamp power W/cm	2	0.0292	0.01459	0.05	0.947
	UV mercury lamp power W/cm	2	0.0677	0.03385	0.13	0.881
	Amount of topcoat	2	13.57	6.7839	34.50	0.000
	Amount of basecoat	2	7.974	3.9872	17.68	0.000
	Number of applicators	1	7.053	7.0528	30.79	0.000
	Type of board	1	0.3694	0.3694	1.40	0.238
	Sandpaper	1	0.6204	0.6204	2.37	0.125
b*	UV LED lamp power W/cm	2	0.0299	0.01497	0.04	0.963
	UV mercury lamp power W/cm	2	0.2822	0.1411	0.36	0.701
	Amount of topcoat	2	24.40	12.2012	44.88	0.000
	Amount of basecoat	2	6.835	3.4175	9.43	0.000
	Number of applicators	1	12.09	12.0884	36.23	0.000
	Type of board	1	0.4319	0.4319	1.10	0.296
	Sandpaper	1	1.759	1.7587	4.55	0.034
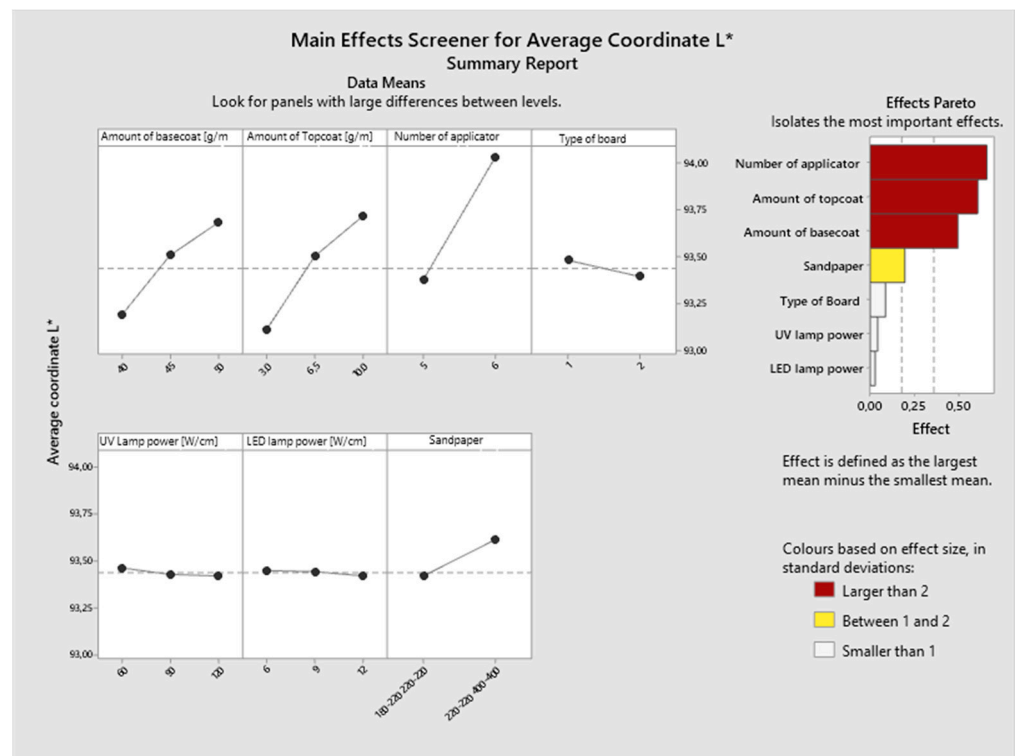
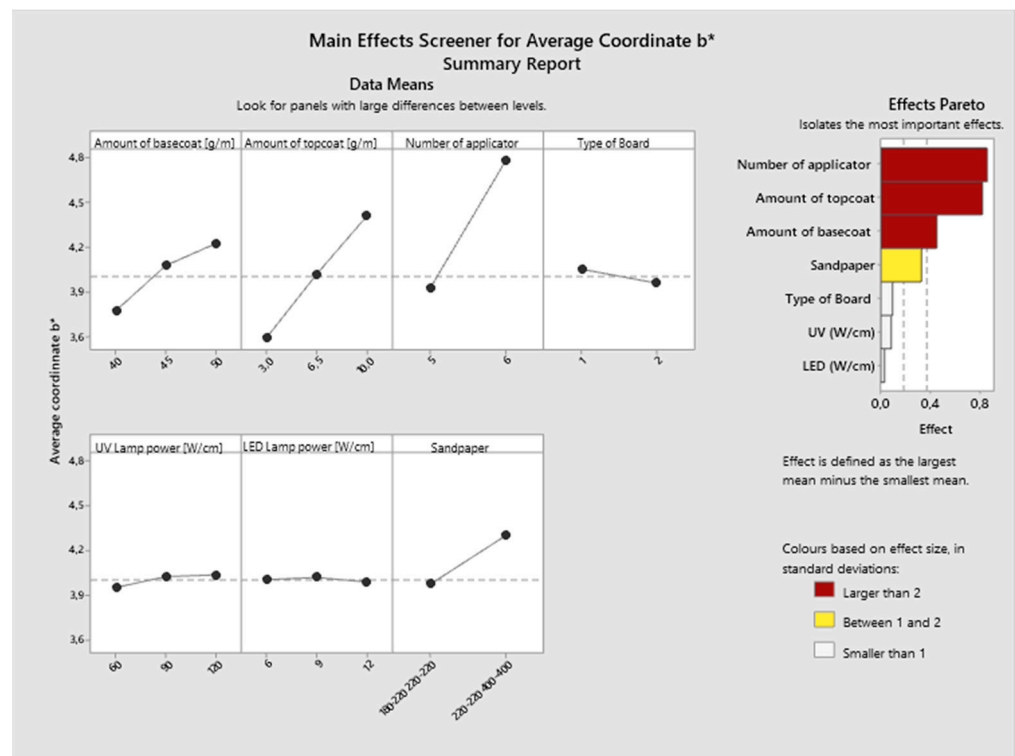**Figure 2.** Main effects and Pareto effects plots for coordinate L*.

Figure 3. Main effects and Pareto effects plots for coordinate b*.

A Pareto analysis was carried out for L* and b* data to account for statistically significant interactions between factors. The results pointed out the following relations: the amount of basecoat–topcoat, basecoat–topcoat–UV mercury lamp power and basecoat–UV mercury lamp power. An interaction plot was then generated to visualize the interactions taking place (Figures 4 and 5). In the case of topcoat–basecoat interaction, the coordinates L* and b* increased when the amount of topcoat and basecoat increased. The largest spread occurred when the smallest assumed amounts of topcoat (3 g/m^2) and basecoat (40 g/m^2) were applied. Moreover, analysing the mercury lamps' power, it is possible to state that increasing the power resulted in a slight increase in L* and b*. The last significant interaction concerns the basecoat and mercury lamp power. The situation was analogous to that described previously, but it was surprising to see a decrease in both L* and b* when applying the largest amount of basecoat tested (50 g/m^2) when cured with a lamp power of 120 W/cm. The results of this variant equated to those obtained for an application of 45 g/m^2 and lamp power of 120 W/cm.

Factorial DOE analysis was carried out for L* and b* data, and optimization plots were generated (Figures 6 and 7). The impact of each factor (columns) on responses or composite efficacy (rows) is shown. The vertical red lines in the graph represent the current ratio settings. The numbers at the top of the column show the current factor level settings (in red). The horizontal blue lines and numbers show the responses for the current factor level. Each impact of the factors on responses or overall desirability is displayed in columns and rows. The graph's current factor settings are shown as vertical red lines. The current factor level settings are indicated (in red) by the numbers at the top of each column. The numbers and horizontal blue lines represent the replies for the current factor level. Based on the obtained data, it was estimated that by increasing the number of overlays in the process, a decrease of the basecoat spread rate from 50 g/m^2 to 40 g/m^2 and of the topcoat from 10 g/m^2 to 4.4 g/m^2 are allowed, when curing with the highest mercury lamp power of 120 W/cm and LED lamp power of 12 W/cm, while maintaining the same high level of coordinate L*. The same relationship applies to coordinate b*. To achieve a high coordinate b* = 4.7815, increasing the number of overlays from 5 to 6 is sufficient, thereby reducing the amount of basecoat applied by 10 g/m^2 and topcoat by 6.2 g/m^2.
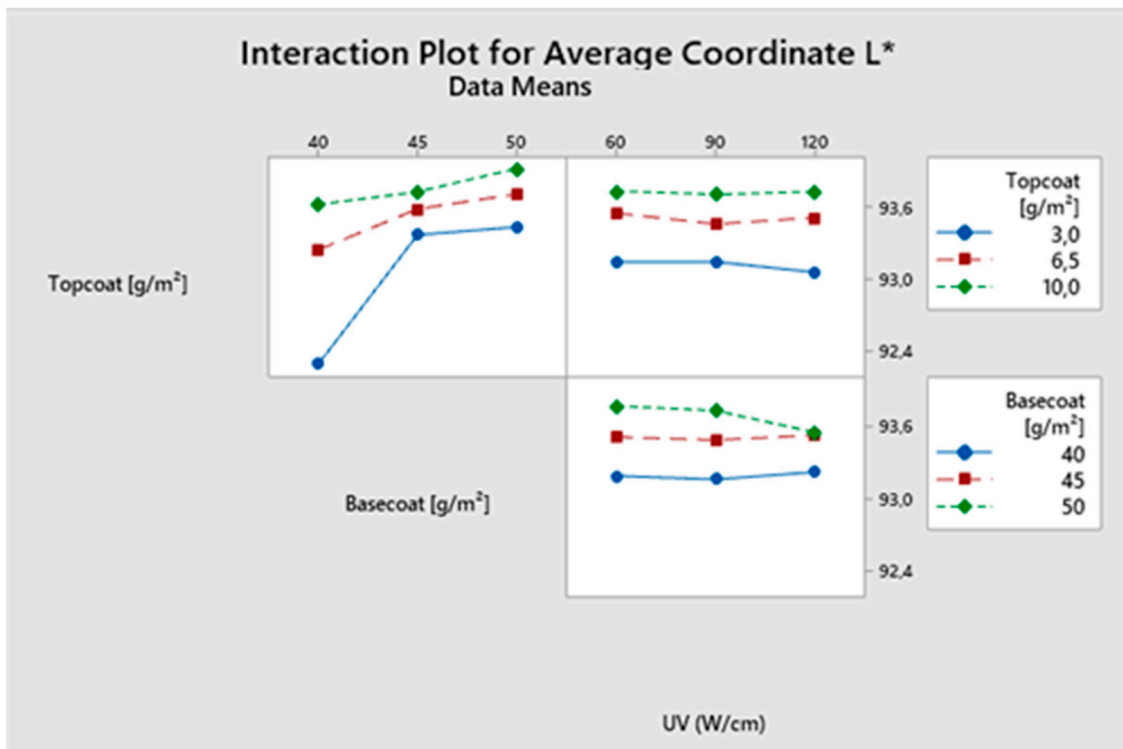
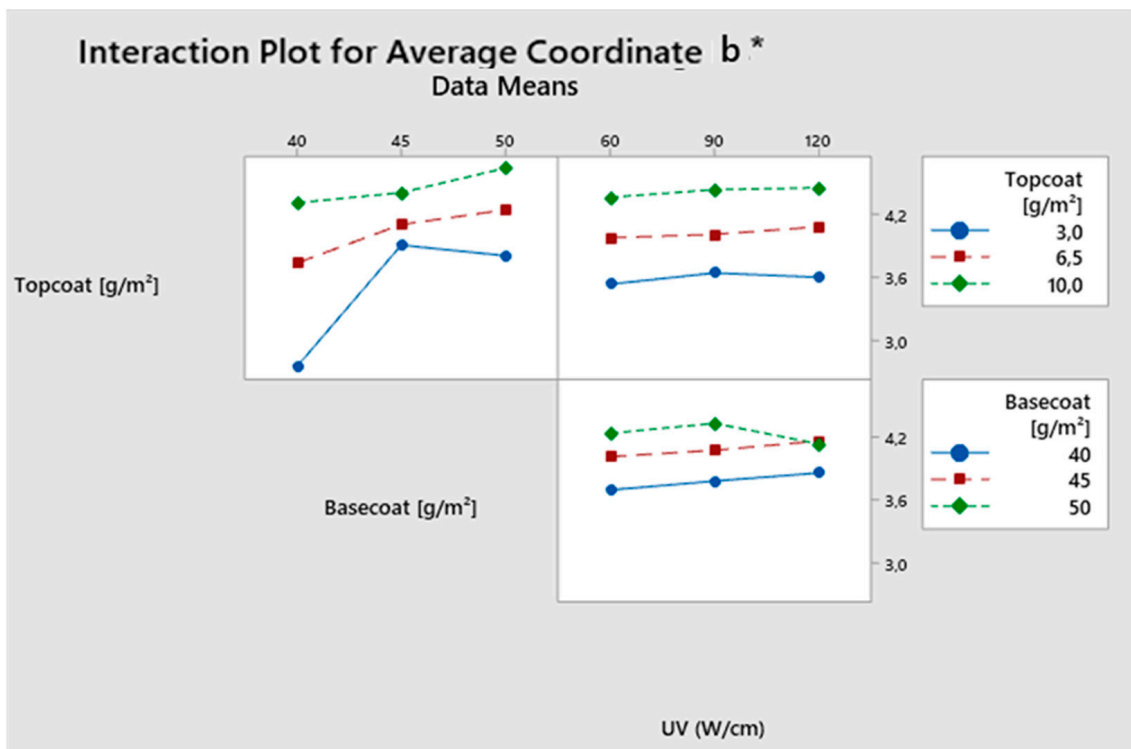**Figure 4.** Interaction plot for coordinate L*.
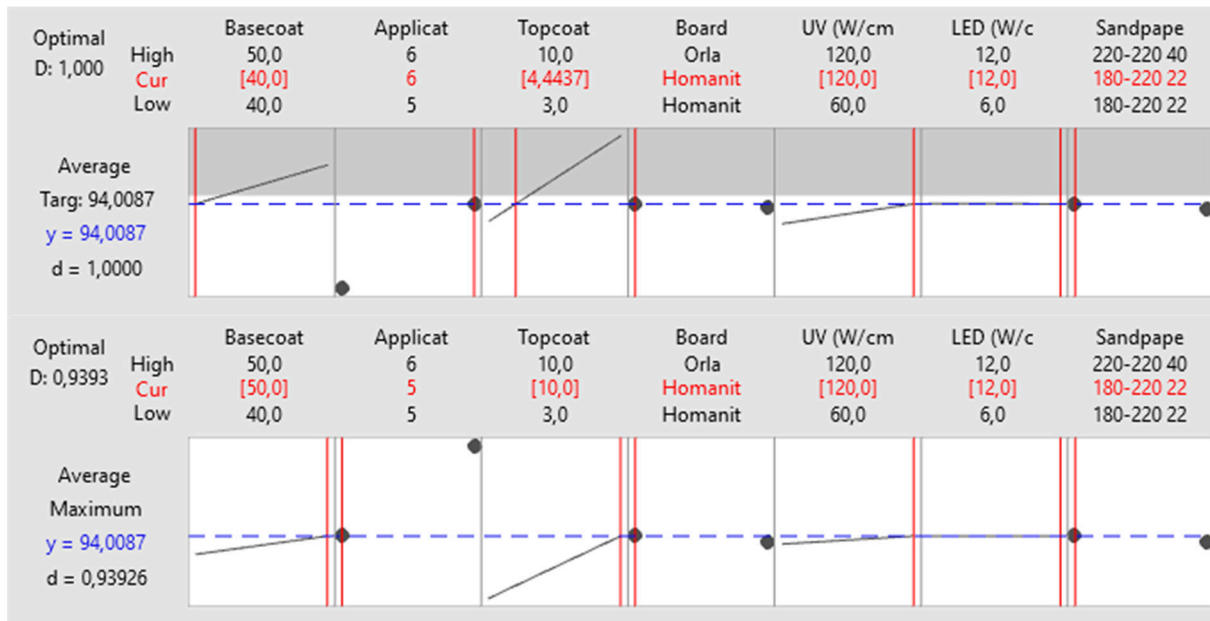

Figure 5. Interaction plot for coordinate b*.
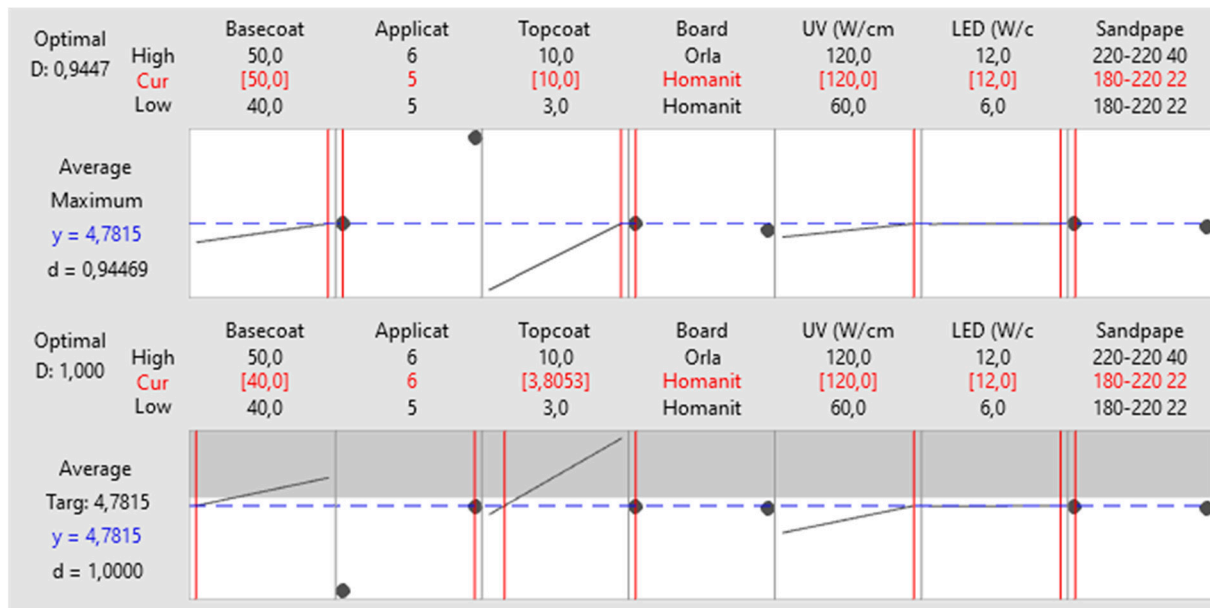
Figure 6. Optimal plot for L*=94,0087.

Figure 7. Optimal plot for b* = 4,7815.

The issue of curing coatings with LED lamps has been pointed out by several researchers, especially in the case of thick layers with a large number of pigments. One avenue has been to improve varnish formulations by changing the amount and type of photoinitiators [36] and developing LED lamps [38]. Another method is to reduce the line speed [36,37]. For floor painting lines, optimum curing is associated with reducing line speed from 9 m/min to 1.5 m/min. A better curing was also indicated for UV water-based formulations than for UV high-solid acrylates [36,37,52]. For thick coatings, hybrid curing is suggested [20]. In the present research, satisfactory coating curing was achieved by using LED and mercury lamps. The observed positive effect of increasing the number of applicators corresponds with the literature data. A better coating quality can be achieved by increasing the number of putty layers on the MDF and using a doctor blade on the application roller [53]. The resulting compromise not only allows a better coating curing,

but also offers the opportunity to save considerable amounts of topcoat and basecoat, as shown in Figures 6 and 7. The increase in coordinates L* and b*, together with the increase in the number of varnishes applied, were related to the varnish properties that provide colour to the painted surface [54].

3.3. Gloss Level

A Pareto effect size plot in standard deviation was determined for the gloss results (Figure 8). It was found that the amount of the applied topcoat, the abrasives used and the number of applicators had the greatest effect on the achieved surface gloss (effect size larger than two). The next two factors are UV mercury lamp power and the amount of the basecoat (between 1 and 2). The type of board and the LED lamp power did not affect this parameter. The main effect plots describe the gloss change direction under individual factors' influence. Applying a topcoat at 3.0 and 6.5 g/m^2 had no significant effect on the analysed ratio. An increase of a further 3.5 g/m^2 resulted in a very sharp increase of almost 10 gloss level units. Using finer abrasive grit size and a greater number of applicators helped increase the recorded gloss values on the coating. Curing with mercury lamps in the intermediate power variant (90 W/cm) resulted in the lowest parameter, while the highest parameter was obtained for 120 W/cm. The gloss decreased as the amount of the basecoat increased. The higher-density HDF board achieved a slightly higher gloss level. The line is horizontal (parallel to the *x*-axis) for LED lamp power, so there was no main effect.
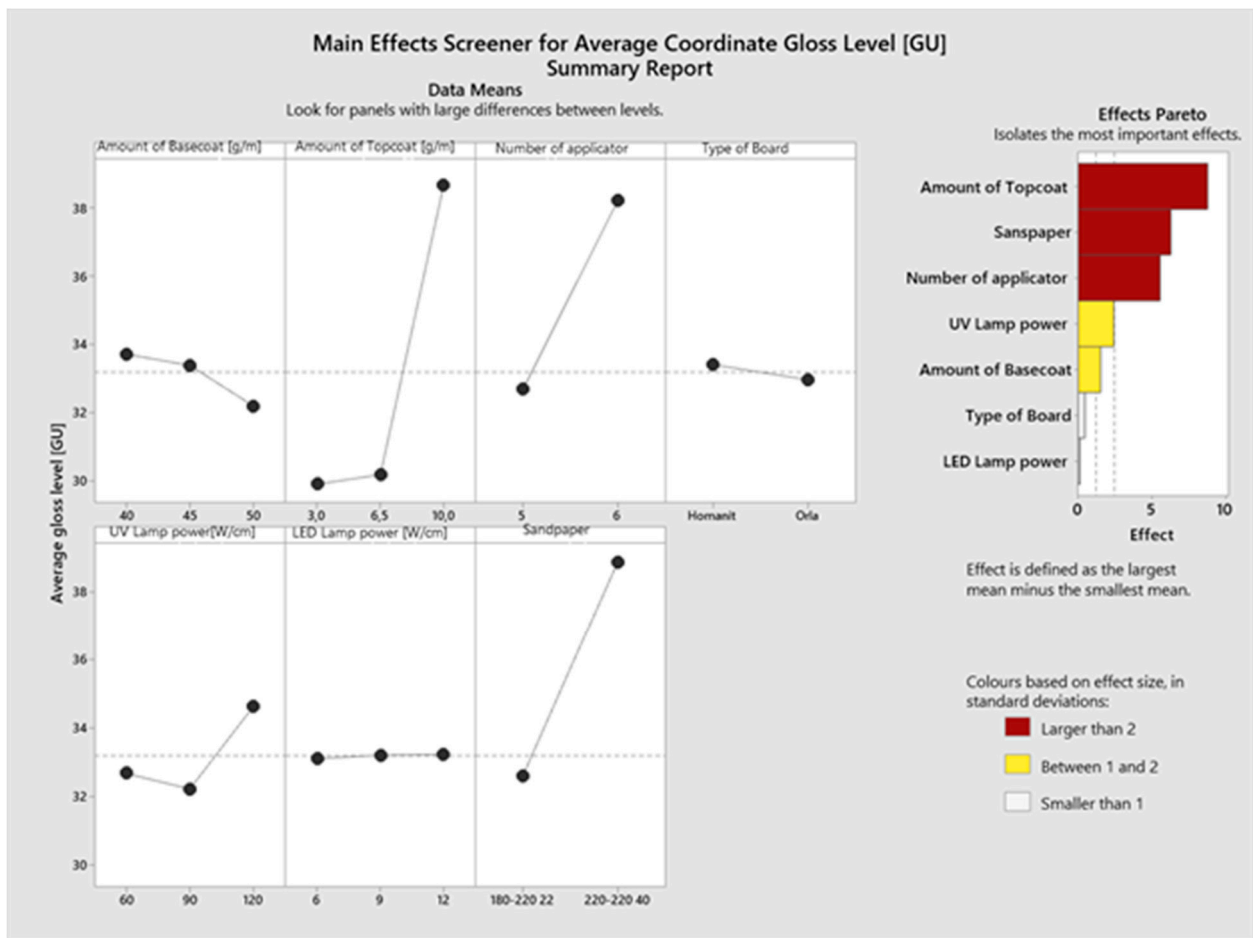

Figure 8. Main effects and Pareto effects plots for gloss level.

Analysing the Pareto chart of the standardized effects for interactions, the only statistically significant interaction was that between the amount of the topcoat applied and mercury lamp power (Figure 9). When 3 g/m^2 of topcoat was applied, the gloss level was

similar for the surfaces cured with mercury lamps at 60 W/cm and 120 W/cm. The lowest values were achieved at 90 W/cm. The gloss level increased by applying 6.5 g/m^2, with the lowest increase recorded for curing with mercury lamps at 60 W/cm. The gloss increased as the lamps' power increased. A further increase for all curing variants proceeded at the same rate.
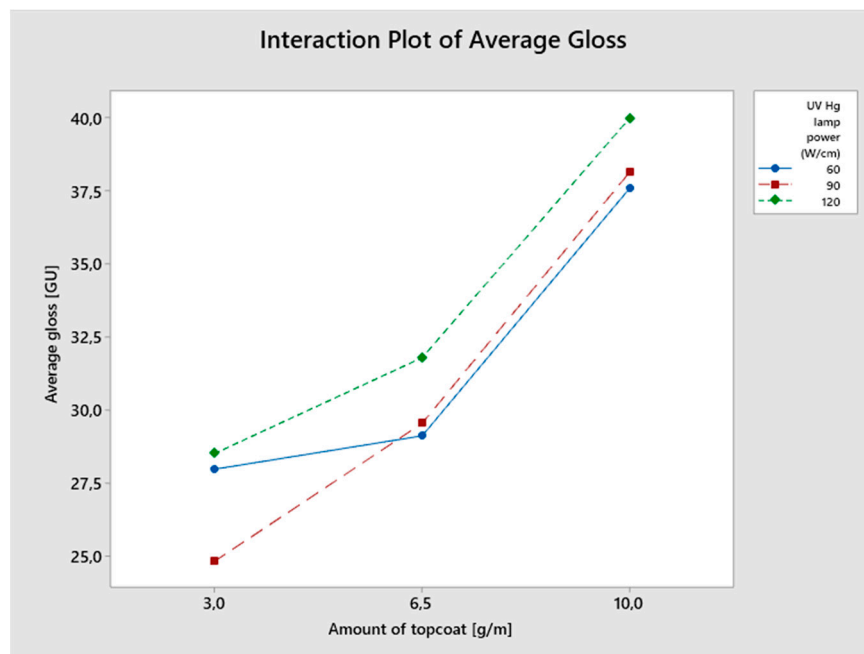
Figure 9. Interaction plot for average gloss level (topcoat–UV mercury lamp power).

Based on these, the author concluded that a thicker coating layer increases the coating resistance. This is consistent with the information provided on quality improvement when more topcoat is applied [54,55]. However, the same principle was not used with the priming varnish. The functions of varnishes need explanations. The basecoat varnish's chemical composition is designed to provide the varnished surface colour, guarantee evenness and provide initial resistance. The fundamental goal of a topcoat is to guarantee a quality finish. According to other reports, the ratios of the materials, the types of resin employed and other additives affect the scratch-resistant coatings [56].

There is a close relationship between the material after grinding and the coating [57], and that was confirmed by determining the effect of grinding on the surface gloss. It has been repeatedly proven that a gloss reduction occurs with an increase in roughness [58,59], which is provided by a smaller material grain size [43,60,61]. Overly aggressive grinding exposes the substrate structure, which can be filled with glue, thereby contributing to a reaction with the applied varnish layer [62]. The roughness of the first basecoat layer increased linearly, and the adhesion decreased for finer abrasives [13]. The cases described confirm the increase in gloss as the abrasive's grain size increased before and after grinding. In the literature, it is also possible to find publications on the increase in gloss with the application of successive varnish coats [45]. Lower gloss was observed with higher topcoat thickness when finishing using conventional UV lamps [55]. This may be due to differences in the composition of varnishes cured by mercury lamps and LED lamps. The researchers also conducted a comparative gloss study after scratch resistance tests of 200 cycles for coatings cured with LED and conventional UV lamps. No difference in gloss loss was noticed between the technologies [52].

The effect of conventional lamp power on colour and gloss of a coating is a common phenomenon known in manufacturing practice [55]. Painting on combined UV mercury and LED lines ensures stable colour and gloss performance. The smaller effect of mercury lamp power and the lack of effect of LED lamps on the test results obtained are a novelty.

This is an additional advantage of LED lamps. The present study will be extended to include testing of the coatings' mechanical resistance to obtain a better coating quality.

4. Conclusions

The scientific contribution of this paper is to present the impact of technological parameters in UV surface refinement using a paint line containing LED and mercury lamps.

In conclusion, this study indicates the intricate relationship between technological and process parameters in UV surface refinement, offering valuable insights into the optimization of paint line processes using LED and mercury lamps. The findings of this research not only contribute to the current body of knowledge, but also hold significant practical implications for the manufacturing and coating industries, particularly in the context of achieving desired colour coordinates and gloss levels. In essence, this study serves as a stepping stone toward a future where UV surface finishing becomes not only more technologically advanced but also environmentally conscious and economically viable.

Based on the results of the study, the following conclusions can be drawn:

- The number of varnish overlays used and the amount of the applied topcoat and basecoat had the greatest impact on colour coordinates L* and b*. Higher coordinates were obtained as the number of overlays and the number of varnishes increased. The interactions between the spread rates of varnish and the mercury lamp power were statistically significant. Increasing the lamp power contributed to the increase in colour coordinates.
- It was estimated that to obtain the highest possible parameter L* = 94., the number of overlays could be increased from 5 to 6, while reducing the amount of the applied basecoat by 10 g/m^2 (from 50 g/m^2 to 40 g/m^2).
- The statistically significant factors affecting the coatings' gloss were the spread rate of the applied topcoat, the abrasive used, the number of coats used and the mercury lamp power used in the process. An increase in gloss occurred with an increase in the spread rate of the applied topcoat, the number of coats and the abrasive grit size. The mercury lamps were also part of a significant interaction with the amount of the topcoat. The gloss increased as the lamps' power and the spread rate of the topcoat increased.
- LED lamp power did not affect the coatings' optical parameters. A high share of LED lamps in the painting line ensures a higher process stability. Moreover, it can be stated that LED lamps still do not affect the coatings' optical parameters, despite the passage of time and the power reduction, which may be a good prognosis for the extension of LED lamp life. It can also represent a large amount of savings due to the high price of LED modules.

Author Contributions: Conceptualisation, M.H. and T.K.; methodology, M.H., B.L. and T.K.; software, M.H.; validation, M.H., B.L. and T.K.; formal analysis, M.H.; investigation, M.H.; resources, M.H., B.L. and T.K.; data curation, M.H.; writing—original draft preparation, M.H., B.L. and T.K.; writing—review and editing, M.H., B.L., E.A.S. and T.K.; visualization, M.H.; supervision, B.L. and T.K.; project administration, B.L. and T.K.; funding acquisition, E.A.S. All authors have read and agreed to the published version of the manuscript.

Institutional Review Board Statement: Not applicable.

Informed Consent Statement: Not applicable.

Data Availability Statement: The data presented in this study are available on request from the corresponding author.

Conflicts of Interest: The authors declare no conflict of interest.

References

1. The Business Research Company. Paints and Coatings Global Market Report 2023. 2023. Available online: https://www.thebusinessresearchcompany.com/report/paints-and-coatings-global-market-report (accessed on 2 November 2023).
2. Kelly, P. European Market Overview 2019. In Proceedings of the RadTech 2020 Conference, Orlando, FL, USA, 8–11 March 2020.
3. ReportLinker. Global Industrial Coatings Market Size, Share & Trends Analysis Report by Product, Technology, End Use, Region, and Segment Forecasts, 2021–2028. 2021. Available online: https://www.marketsandmarkets.com/Market-Reports/industrial-coatings-market-746.html (accessed on 2 November 2023).
4. Raport. Nowy raport przewiduje wzrost na globalnym rynku powłok przemysłowych [New report predicts growth in global industrial coatings market]. *Lakiernictwo Przemysłowe* **2022**, *1*, 135. Available online: https://www.lakiernictwo.net/dzial/142-aktualnosci-i-przeglad-rynku/artykuly/nowy-raport-przewiduje-wzrost-na-globalnym-rynku-p,4819 (accessed on 2 November 2023).
5. Jabłoński, M.; Świetliczny, M.; Ružińska, E. *Polimery Syntetyczne i Materiały Malarsko-Lakiernicze w Myślach Drzewnym [Synthetic Polymers and Paint and Varnish Materials in the Woodworking Industry]*; Wydawnictwo SGGW: Warsaw, Poland, 2009.
6. Marasinghe, L.; Croutxé-Barghorn, C.; Allonas, X.; Criqui, A. Effect of reactive monomers on polymer structure and abrasion resistance of UV cured thin films. *Prog. Org. Coat.* **2018**, *118*, 22–29. [CrossRef]
7. Weber, E. North American UV+EB Market Overview. In Proceedings of the RadTech 2020 Conference, Orlando, FL, USA, 8–11 March 2020; Available online: www.radtech.org (accessed on 2 November 2023).
8. Cano, M.; Núñez-Lozano, R.; Lumbreras, R.; González-Rodríguez, V.; Delgado-García, A.; Jiménez-Hoyuela, J.M.; de la Cueva-Méndez, G. Partial PEGylation of superparamagnetic iron oxide nanoparticles thinly coated with amine-silane as a source of ultrastable tunable nanosystems for biomedical applications. *Nanoscale* **2017**, *9*, 812–822. [CrossRef]
9. Jung, S.J.; Lee, S.J.; Cho, W.J.; Ha, C. Synthesis and properties of UV-curable waterborne unsaturated polyester for wood coating. *J. Appl. Polym. Sci.* **1998**, *69*, 695–708. [CrossRef]
10. Heuer, A.M.; Reinartz, R.; Skotarczak, A.; Presenter, M.N.; Lin, B. Novel approaches to improve scratch and abrasion resistance in UV coatings. In Proceedings of the RadTech 2020 Conference, Orlando, FL, USA, 8–11 March 2020.
11. Curatolo, B. UV technology for the protection of surfaces. *UV+ EB Technol.* **2015**, *2*, 22–29.
12. Li, Y.; Shao, H.; Lv, P.; Tang, C.; He, Z.; Zhou, Y.; Shuai, M.; Mei, J.; Lau, W.M. Fast preparation of mechanically stable superhydrophobic surface by UV cross-linking of coating onto an oxygen-inhibited layer of substrate. *Chem. Eng. J.* **2018**, *338*, 440–449. [CrossRef]
13. Guo, X.; Li, R.; Teng, Y.; Cao, P.; Wang, X.A.; Ji, F. Effects of surface treatment on the properties of UV coating. *Wood Res.* **2015**, *60*, 629–638.
14. Lustig, C.; Chakrapani, S. UV curable coatings-options for challenging substrates. In Proceedings of the RadTech 2020 Conference, Orlando, FL, USA, 8–11 March 2020.
15. Wnuk, R. Wodne materiały utwardzające promieniowaniem UV-przyszłość w lakierowanie drewna. *Uszlachetnianie Powierzchni Drzewnych cz. II.* 2011, pp. 16–18. Available online: https://woodchem.pl/uszlachetnianie-powierzchni-drewna/ (accessed on 2 November 2023).
16. Heathcote, J. Update on Mercury Regulation for UV Curing Lamps. In Proceedings of the RadTech 2020 Conference, Orlando, FL, USA, 8–11 March 2020.
17. Borysiuk, P.; Derda, M.; Auriga, R.; Boruszewski, P.; Monder, S. *1. Comparison of Selected Properties of Varnish Coatings Curing with the Use of UV and UV-LED Approach*; Annals of Warsaw University of Life Sciences—SGGW Forestry and Wood Technology: Warsaw, Poland, 2015; ISSN 1898-5912.
18. Studer, K.; Decker, C.; Beck, E.; Schwalm, R. Overcoming oxygen inhibition in UV-curing of acrylate coatings by carbon dioxide inerting, Part I. *Prog. Org. Coat.* **2003**, *48*, 92–100. [CrossRef]
19. Taki, K.; Yamada, R. Comparison of the degree of shrinkage under air and nitrogen atmospheres by laser displacement sensor. *J. Photopolym. Sci. Technol.* **2018**, *31*, 497–501. [CrossRef]
20. Park, J.W.; Sim, K.B.; Shim, G.S.; Back, J.H.; Baek, D.; Kim, H.J.; Shin, S. Depth profile of thin coating through surface and interfacial cutting analysis of UV curing system. *Mater. Des.* **2019**, *178*, 107855. [CrossRef]
21. Wang, T.; Shaw, J. Physical Properties of UV Curable Composites. In Proceedings of the RadTech 2020 Conference, Orlando, FL, USA, 8–11 March 2020; Available online: www.allnex.com (accessed on 2 November 2023).
22. Rudnicki, A. Lakiery utwardzane promieniami UV-wiele zalet [UV-cured varnishes—Many advantages]. *Lakiernictwo Przemysłowe. Uszlachetnianie Powierzchni Drzewnych cz. III.* 2011, pp. 16–17. Available online: https://woodchem.pl/uszlachetnianie-powierzchni-drewna/ (accessed on 2 November 2023).
23. Kien, W.; Osajda, M.; Boratyński, P. Linie lakiernicze z utwardzaniem naskórka promieniami UV-dobierz temperaturę urządzenia [Paint lines with UV surface curing—Adjust the device temperature]. *Lakiernictwo Przemysłowe. Uszlachetnianie Powierzchni Drzewnych cz. V.* 2013, pp. 40–47. Available online: https://woodchem.pl/uszlachetnianie-powierzchni-drewna/ (accessed on 2 November 2023).
24. Wnuk, R.; Utwardzanie powłoki lakierniczych przy użyciu LED. Utwardzanie powłoki lakierniczych przy użyciu LED. Oszczędne i „pożerające" mniej energii" [LED paint curing. Economical and consuming less energy]. *Lakiernictwo Przemysłowe. Uszlachetnianie Powierzchni Drzewnych cz. V.* 2013, pp. 34–35. Available online: https://woodchem.pl/uszlachetnianie-powierzchni-drewna/ (accessed on 2 November 2023).

25. Wang, X.; Feng, Y.; Zhang, L.; Protsak, I.; Jamali, R.; Shu, Y.; Pal, P.; Wang, Z.; Yang, J.; Zhang, D. Fast-cured UV-LED polymer materials filled with high mineral contents as wear-resistant, antibacterial coatings. *Chem. Eng. J.* **2020**, *382*, 122927. [CrossRef]

26. Heathcote, J. Update on Mercury Regulation for UV Curing Lamps. GEW (EC). 6 March 2023. Available online: https://www.pffc-online.com/news/17269-update-on-mercury-regulation-for-uv-curing-lamps (accessed on 1 May 2023).

27. European Commission. RoHS 2 FAQ. 2012. Available online: http://ec.europa.eu/enterprise/policies/single-market-goods/documents/blue-guide/ (accessed on 2 November 2023).

28. European Commission. *Fact Sheet Questions and Answers: EU Mercury Policy and the Ratification of the Minamata Convention*; European Commission: Brussels, Belgium, 2017.

29. United Nations Environment Programme. Minamata Convention on Mercury Text and Annexes. 2019. Available online: www.mercuryconvention.org (accessed on 2 November 2023).

30. Minamata Convention on Mercury. Strengthening the Specific International Programme to Support Capacity-Building and Technical Assistance of the Minamata Convention on Mercury: Enhancing the Effective Functioning of the Programme. 2021. Available online: https://minamataconvention.org/en/implementation/specific-international-programme (accessed on 2nd November 2023).

31. Beutler, P. 4. Mercury-Vapor Lamp or LED? Karlsruhe. 2022. Available online: http://assets.thermofisher.com/TFS-Assets/MSD/Product-Information/mercury-vapor-lamp-led-en-p072.pdf (accessed on 30 April 2023).

32. Kiyoi, E. 3. Keep It Cool to Keep It Clean Advantages of UV LEDs When Coating Heat-Sensitive Types of Wood. 2013. Available online: www.european-coatings.com (accessed on 2 November 2023).

33. Kiyoi, E. 5. The State of UV-LED Curing: An Investigation of Chemistry and Applications Characteristics of UV-LED Lamps. 2013. Available online: https://radtech.org (accessed on 2 November 2023).

34. Bekas, J. Skuteczniej utwardzają, a nie podgrzewają. *Gaz. Przemysłu Drzewnego* **2015**, *9*, 45.

35. Dawidowicz, A.L.; Nowakowski, P.; Dybowski, M.P.; Typek, R. Some physicochemical properties of polyacrylate varnish layers cured by classical and LED (395 nm) UV sources. *Food Packag. Shelf Life* **2020**, *24*, 100497. [CrossRef]

36. Europen Coatings. Radiation curing by LED technology for industrial wood flooring coatings. *Focus Powder Coat.* **2023**, *2023*, 6. [CrossRef]

37. Goodrich, J.E. Acrylated Amine Oligomers to Enhance Cure with UV LED Sources. In Proceedings of the RadTech 2020 Conference, Orlando, FL, USA, 8–11 March 2020.

38. Schmitz, C.; Poplata, T.; Feilen, A.; Strehmel, B. Radiation crosslinking of pigmented coating material by UV LEDs enabling depth curing and preventing oxygen inhibition. *Prog. Org. Coat.* **2020**, *144*, 105663. [CrossRef]

39. Ivarsson, D. The Impact of Different Intensities on the Performance of Led Cured Coatings. Available online: https://www.pcimag.com (accessed on 2 November 2023).

40. Gharagozloo, M.; Dombkowski, T.; Leonhardt, D.; Xu, D.; Macairan, J.; Skinner, B. IIoT Enabled Smart UV Systems. In Proceedings of the RadTech 2020 Conference, Orlando, FL, USA, 8–11 March 2020.

41. Ivarsson, D.; Bilinsky, H. Curing matt finishes into UV curable wood coatings by direct contactless microfabrication. In Proceedings of the RadTech 2020 Conference, Orlando, FL, USA, 8–11 March 2020.

42. Salca, E.A.; Krystofiak, T.; Lis, B.; Hiziroglu, S. Glossiness evaluation of coated wood surfaces as function of varnish type and exposure to different conditions. *Coatings* **2021**, *11*, 558. [CrossRef]

43. Salca, E.A.; Krystofiak, T.; Lis, B.; Mazela, B.; Proszyk, S. Some coating properties of black alder wood as a function of varnish type and applications method. *Bioresources* **2016**, *11*, 7580–7594. [CrossRef]

44. Jančovičová, V.; Kindernay, J.; Jakubíková, Z.; Mrlláková, I. Influence of photoinitiator and curing conditions on polymerization kinetics and gloss of UV-cured coatings. *Chem. Pap.* **2007**, *61*, 383–390. [CrossRef]

45. Gürleyen, L. Effects of artificial weathering on the colour, gloss, adhesion, and pendulum hardness of UV system parquet varnish applied to doussie (Afzelia africana) wood. *Bioresources* **2021**, *16*, 1616–1627. [CrossRef]

46. Okamura, H.; Niizeki, S.; Ochi, T.; Matsumoto, A. UV curable formulations for UV-C LED. *J. Photopolym. Sci. Technol.* **2016**, *29*, 99–104. [CrossRef]

47. *ISO 2813*; Paints and Varnishes—Determination of Specular Gloss of Non-Metallic Paint Films at 20 Degrees, 60 Degrees and 85 Degrees. International Organization for Standardization: Geneva, Switzerland, 1994.

48. *DIN 67530*; Reflectometer as a Means for Gloss Assessment of Plane Surfaces of Paint Coatings and Plastics. European Standards: Brussels, Belgium, 1982.

49. *ISO 7724*; Paints and Varnishes. Colourimetry. Part 2: Colour Measurement. International Organization for Standardization: Geneva, Switzerland, 1984.

50. Hill, B.; Roger, T.; Vorhagen, F.W. Comparative Analysis of the Quantization of Colour Spaces on the Basis of the CIELAB Colour-Difference Formula. *ACM Trans. Graph.* **1997**, *16*, 109–154. [CrossRef]

51. Wijekularathna, S.M.; Manage, D.K.; Scariano, A.B.W. Power analysis of several normality tests: A Monte Carlo simulation study. *Commun. Stat. Simul. Comput.* **2020**, *51*, 757–773. [CrossRef]

52. Landry, V.; Blanchet, P.; Boivin, G.; Bouffard, J.F.; Vlad, M. UV-LED curing efficiency of wood coatings. *Coatings* **2015**, *5*, 1019–1033. [CrossRef]

53. Evans, P.D.; Cullis, I. Effect of sanding and coating with UV-cured finishes on the surface roughness, dimensional stability and fire resistance of oriented strandboard. *Holz als Roh-und Werkstoff* **2008**, *66*, 191–199. [CrossRef]

54. Akkuş, M.; Akbulut, T.; Candan, Z. Application of electrostatic powder coating on wood composite panels using a cooling method. Part 1: Investigation of water intake, abrasion, scratch resistance, and adhesion strength. *BioResources* **2019**, *14*, 9557–9574. [CrossRef]
55. Henke, M.; Lis, B.; Krystofiak, T. Gloss Level of HDF Finished with Different Numbers of Layers and Hardened with UV Hg-Ga Lamps of Selected Power. *Coatings* **2022**, *12*, 533. [CrossRef]
56. Lis, B.; Krystofiak, T.; Proszyk, S. Studies of the resistance upon some factors of UV acrylic lacquer coatings on MDF boards. Part II. Mechanical factors. *Ann. Warsaw Univ. Life Sci. SGGW For. Wood Technol.* **2010**, *71*, 454–457.
57. Bekhta, P.; Lis, B.; Krystofiak, T.; Bekhta, N. Surface Roughness of Varnished Wood Pre-Treated Using Sanding and Thermal Compression. *Forests* **2022**, *13*, 777. [CrossRef]
58. Qi, L.; Chantler, M.J.; Siebert, P.; Dong, J. The joint effect of mesoscale and microscale roughness on perceived gloss. *Vis. Res.* **2015**, *115*, 209–217. [CrossRef] [PubMed]
59. Honson, V.; Huynh-Thu, Q.; Arnison, M.; Monaghan, D.; Isherwood, Z.J.; Kim, J. Effects of Shape, Roughness and Gloss on the Perceived Reflectance of Coloured Surfaces. *Front. Psychol.* **2020**, *11*, 485. [CrossRef] [PubMed]
60. de Moura, L.F.; Brito, J.O.; Nolasco, A.M.; Uliana, L.R. Evaluation of coating performance and colour stability on thermally rectified Eucalyptus grandis and Pinus caribaea var. Hondurensis woods. *Wood Res.* **2013**, *58*, 231–242.
61. Sinn, G.; Ginkl, M.; Reiterer, A.E.T.; Stanzl-Tschegg, S. Changes in the surface properties of wood due to sanding. *Holzforschung* **2004**, *58*, 246–251. [CrossRef]
62. Zeren, S.; Huguenard, S. UV-curable powder coatings: Formulation of thick white finish for MDF. *Surf. Coat. Int. Part B Coat. Trans.* **2004**, *87*, 71–148. [CrossRef]